F. Méot
Brookhaven Nal Lab.

HRS-DESIR Review Committee
CEN-Bordeaux Gradignan
17-18 November 2011

SPIRAL2/DESIR High Resolution Spectrometer
A review of Zgoubi-based simulation methods

Plans :

- I discuss various of the ways to simulate HRS bends, comment on some of the results so obtained
- I go over some of the simulations Laurent gave me to review

1 Introduction

Numerical simulations shown here assume the following :

- $B\rho = 0.405179$ T.m, mass=122957.21 eV, which corresponds to ^{132}Sn$^+$, 60 keV kinetic energy, $\beta = 0.987901\,10^{-3}$.

- Electrostatic quadrupoles are simulated using a multipole analytical model, “ELMULT”.
  Fringe fields coefficients in quadrupoles are :
  $C_0 - C_5 =$ 0.296471, 4.533219, -2.270982, 1.068627, -0.036391, 0.022261.

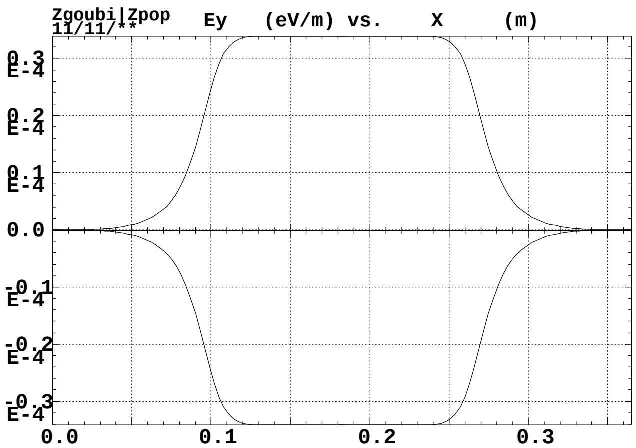

Figure 1: Electric field component E_Y (transverse horizontal) along MQ1, MQ2, as experienced at Y=1 mm (aperture diameter is 4 cm). Note : this is unchanged compared to previous, Nov. 2009's, simulation data. Field fall-off characteristic length in Zgoubi is $\lambda = 4$ cm.

```
 'ELMULT'                MQ1
0
18.5 2. 0. -6.77193263E2 0. 0. 0. 0. 0. 0. 0. 0.
9. 4. 0. 0. 0. 0. 0. 0. 0. 0. 0.
6 .29647 4.53321 -2.27098 1.06862 -0.03639 0.02226
9. 4. 0. 0. 0. 0. 0. 0. 0. 0. 0.
6 .29647 4.53321 -2.27098 1.06862 -0.03639 0.02226
0. 0. 0. 0. 0. 0. 0. 0. 0. 0.
#60|30|60
1  0. 0. 0.
```

$$FF = \frac{1}{1 + \exp(C_0 + C_1 \frac{d}{\lambda} + C_2 \left(\frac{d}{\lambda}\right)^2 + ... + C_5 \left(\frac{d}{\lambda}\right)^5)}$$

• HRS bends can be simulated using “BEND”, with either “hard edge” field

• or with fringe fields. In that case with Enge coefficients
$C_0 - C_5 =$ 0.498959, 1.911289, -1.185953, 1.630554, -1.082657, 0.318111.

that yield fringe fall-off comparable to field map’s, Figure below.

• HRS bends can be simulated using “TOSCA” that can handle 2D (here) or 3D magnetic field maps

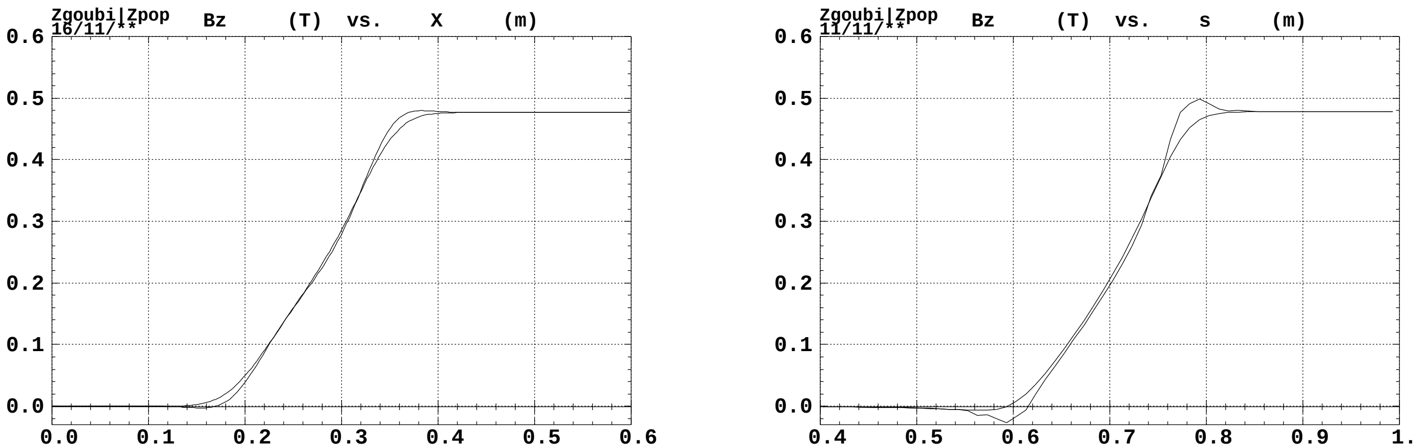

Figure 2: Field along reference orbit in mid-plane and at z=3 cm elevation, in magnet entrance region.
• Left : “BEND” with Enge coefficients $C_0 - C_5 =$ 0.498959, 1.911289, -1.185953, 1.630554, -1.082657, 0.318111. and $\lambda = 10$ cm, entrance and exit integration extent is 30 cm.
• Right : Field map using “TOSCA” procedure.

• HRS bends can be simulated using “DIPOLE”, a powerful numerical method (GANIL’s SPEG, SATURNE, PS spectrometers) that uses the magnet geometry (location and orientation of field boundaries) to “invent” mid-plane field at particle location. Extrapolation off mid-plane by Taylor/Maxwell series.

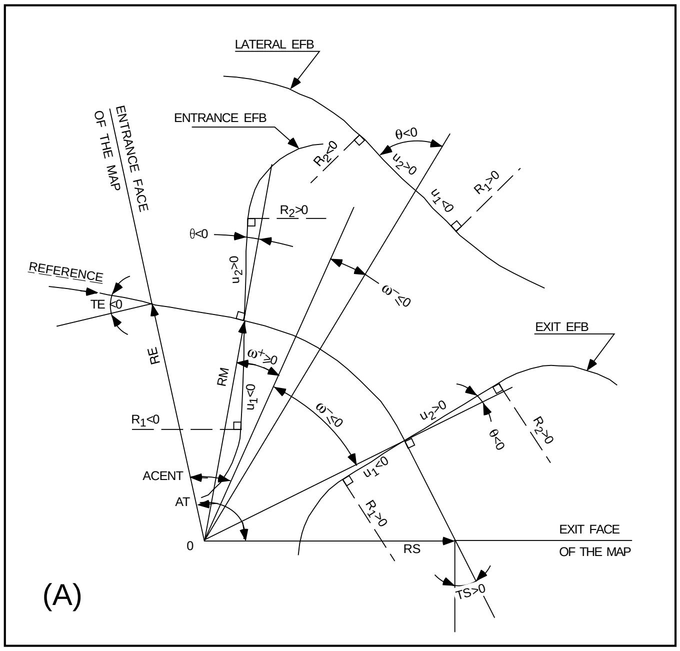

Figure 3: Simulation of the bends using “DIPOLE”.

```
 'DRIFT'                                                        7
-30.
 'DIPOLE'                                                       8
0
128.880069656   85.                          AT, RM
64.440034828 4.76681176471 0. 0. 0.         ACNT, B0, indices
10. -1.
6  -4.2366E-01 2.3175E+00 -1.2644E+00 1.0555E+00 0. 0. 0.
45.  36.   1.E6  -1.E6  1.E6  1.E6
10. -1.
6  -4.2366E-01 2.3175E+00 -1.2644E+00 1.0555E+00 0. 0. 0.
-45.  -36.   1.E6  -1.E6  1.E6  1.E6
0. 0.
0  0.      0.      0.      0.      0. 0.  0.
0.  0.   0.    0.    0. 0. 0.
2   20.
.2
2  90.1387818866  -0.339292614454  90.1387818866  0.339292614454
 'DRIFT'                                                        9
-30.
```

• Note 1 : the “DIPOLE-M” version *generates a 2D field map*, thus interpolating field at particle from the 2D mesh.
• Note 2 : “BEND” data list, for comparison :

```
 'BEND'                                                         2
2
120.2081528  0.  4.76681176471        !!!!4.7687536
30. 10.    0.62831853
6  -4.2366E-01 2.3175E+00 -1.2644E+00 1.0555E+00 0. 0.
30. 10.     0.62831853
6  -4.2366E-01 2.3175E+00 -1.2644E+00 1.0555E+00 0. 0.
.4
3  0.  0.  -0.7853981633
```

• Interest of the “DIPOLE” method :
• Allows sextupole, octupole and decapole transverse indices.
• Allows entrance and exit face curvatures (sextupole-, octupole-like)
• Allows optimizing those parameters using the “FIT” procedure

• Just to figure out... GSI's KAOS using "DIPOLE".

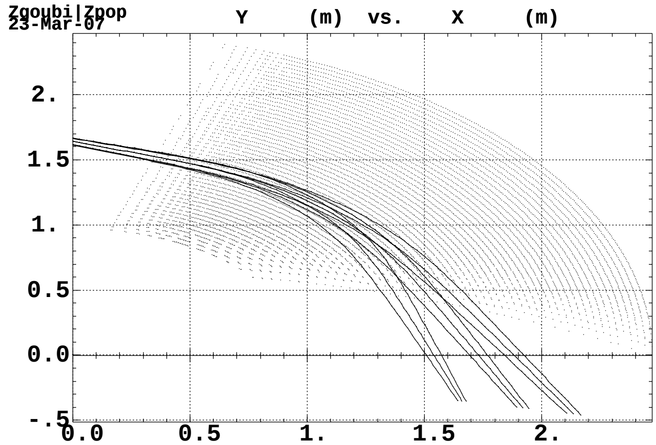

Figure 4: KAOS 750 MeV/c QD spectrometer, iso-field lines and trajectories in dipole.

• Comparing transport matrices through "BEND" (top) and through "DIPOLE" (middle) :

```
Reference particle (# 1), path length :   131.50552     cm  relative momentum :        1

     0.747628        0.823608          0               0               0            0.812866
    -0.535513        0.747628          0               0               0            1.72484
         0               0          2.076669E-02    1.40171            0               0
         0               0         -0.713104       2.07667E-02         0               0
     1.72484         0.812867          0               0               1            0.513889

          DetY-1 =       0.0000000247,    DetZ-1 =       0.0000000196

   ----------------------

Reference particle (# 1), path length :   131.50553     cm  relative momentum :        1

     0.747615        0.823612          0               0               0            0.812867
    -0.535524        0.747626          0               0               0            1.72484
         0               0          2.077162E-02    1.40171            0               0
         0               0         -0.713105       2.076542E-02        0               0
     1.72482         0.812870          0               0               1            0.513889

          DetY-1 =       0.0000000189,    DetZ-1 =       0.0000000072

   ----------------------
```

Note the difference with theoretical value in the hard edge model, as induced by fringe fields :

$r11 = \frac{\cos(\phi-\alpha)}{\cos(\alpha)} = \mathbf{0.72654}$ $\quad r12 = r * \sin\phi = \mathbf{0.85}$ $\quad r13 = r * (1-\cos\phi) = \mathbf{0.85}$

$r21 = -\frac{\sin(\phi-\alpha-\beta)}{\cos(\alpha)\cos(\beta)}/r = \mathbf{-0.55545}$ $\quad r22 = \frac{\cos(\phi-\beta)}{\cos(\beta)} = \mathbf{0.72654}$ $\quad r23 = \sin\phi + (1-\cos\phi)\tan(\beta) = \mathbf{1.7265}$

$r33 = 1 - \phi * \tan(\alpha) = \mathbf{-0.14125}$ $\quad r34 = r\phi = \mathbf{1.3351}$

$r43 = (-\tan(\alpha) - \tan(\beta) + \phi * \tan(\alpha)\tan(\beta))/r = \mathbf{-0.73402}$ $\quad r44 = 1 - \phi * \tan(\beta) = \mathbf{-0.14125}$

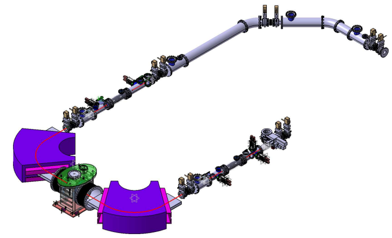

2 Reference theoretical design, hrs_u180_v5.dat

Simulations shown here use data files communicated by Laurent.

2.1 Quadrupole doublet

Here I compute the transport coefficients 1.165 meter downstream of the object. Zgoubi input data file is given in page 11.

R12 and R34 are constrained to 0, yielding potentials in

$$MQ1/-705.5, \quad MQ2/+816.4$$

with the fringe field conditions above.

The transport conditions so obtained are :

```
Reference particle (# 1), path length :   116.50000     cm  relative momentum :       1

                  TRANSFER  MATRIX  ORDRE  1  (MKSA units)

-0.218719          0               0               0             0         0
-8.12638        -4.57208           0               0             0         0
    0              0            -2.73607           0             0         0
    0              0            -6.80265        -0.365488        0         0
    0              0               0               0             1.           0

          DetY-1 =      -0.0000003696,    DetZ-1 =      -0.0000003694

      First order symplectic conditions (expected values = 0) :
        -3.6962E-07   -3.6944E-07    5.2728E-17    3.0424E-17   -3.8982E-16   -1.0792E-16
```

Hard edge, for comparison

The potentials necessary for obtaining R12=R34=0 in the case of hard-edge quadrupole models, would be

$$MQ1/-697.9, \quad MQ2/+807.4$$

which means a small $\sim 1\%$ tuning difference compared to the above. The ensuing first order transport conditions are very close to the fringe field case ones :

```
Reference particle (# 1), path length :   116.50000     cm  relative momentum :       1

                  TRANSFER  MATRIX  ORDRE  1  (MKSA units)

     -0.220325          0                0                0              0         0
     -8.05261       -4.53874             0                0              0         0
         0              0           -2.71379              0              0         0
         0              0           -6.73080         -0.368487           0         0
         0              0                0                0              1.        0.
         0              0                0                0              0.        1.

          DetY-1 =      -0.0000035741,    DetZ-1 =      -0.0000035744

      First order symplectic conditions (expected values = 0) :
        -3.5741E-06   -3.5744E-06   -1.0519E-16   -5.8989E-17   -1.8304E-16   -1.3469E-16
```

SOFT EDGE :

```
Reference particle (# 1), path length :   116.50000     cm  relative momentum :       1

                  TRANSFER  MATRIX  ORDRE  1  (MKSA units)

-0.218719          0                0                0              0         0
-8.12638       -4.57208             0                0              0         0
    0              0           -2.73607              0              0         0
    0              0           -6.80265         -0.365488           0         0
    0              0                0                0              1.           0

          DetY-1 =      -0.0000003696,    DetZ-1 =      -0.0000003694

      First order symplectic conditions (expected values = 0) :
        -3.6962E-07   -3.6944E-07    5.2728E-17    3.0424E-17   -3.8982E-16   -1.0792E-16
```

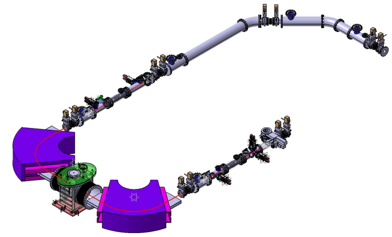

Concluding on MQ1, MQ2 :

Fig. 5 shows the behavior of four particular rays across the doublet.

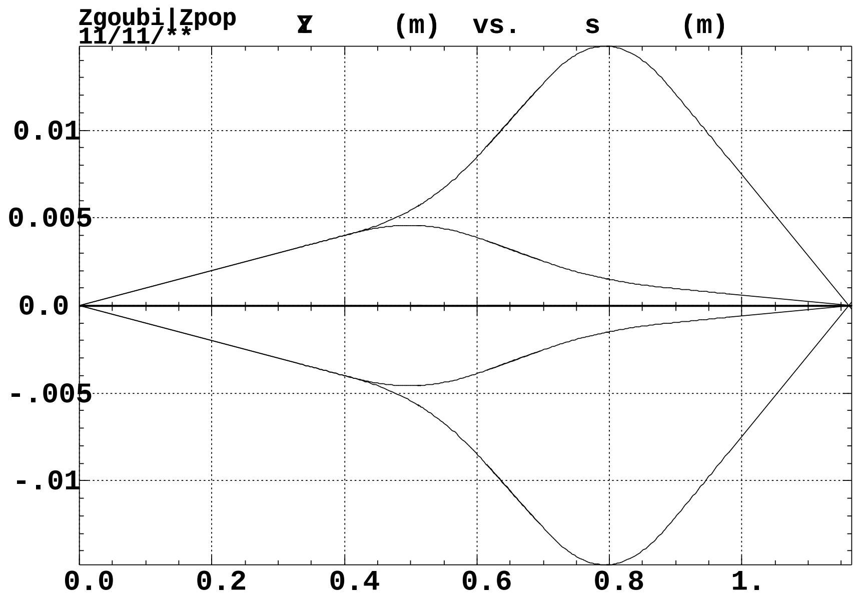

Figure 5: Four trajectories leaving the object with $Y_0' = Z_0' = \pm 10$ mrad.

Quadrupole doublet, soft edge, zgoubi data file

The data list includes FIT procedure for possibly improving further $R_{12} = R_{34} = 0$ at double focus.

```
hrsdesir U180_V6t3
 'OBJET'
  405.179    (Sn132+, 60 KeV)
  5
 0.001  .001  0.001  .001  .001  .0001           changed :  rays have to be paraxial
 0.  0.  0.  0.  0.  1.
'PARTICUL'         2
  122957.21  1.602176487E-19 0.0 0.0 0.0
'MARKER'
'DRIFT'
  42.
  'ELMULT'MQ1
  0
  18.5 2. 0. -705.5 0. 0. 0. 0. 0. 0. 0. 0.
  9. 4. 1. 0. 0. 0. 0. 0. 0. 0. 0.
  6  .296471 4.533219 -2.270982 1.068627 -0.036391 0.022261
  9. 4. 1. 0. 0. 0. 0. 0. 0. 0. 0.
  6  .296471 4.533219 -2.270982 1.068627 -0.036391 0.022261
  0. 0. 0. 0. 0. 0. 0. 0. 0. 0.
  #60|30|60
  1  0. 0. 0.
  'DRIFT'
  10.00
'ELMULT'MQ2
  0
  18.5 2. 0. +816.4  0. 0. 0. 0. 0. 0. 0. 0.
  9. 4. 1. 0. 0. 0. 0. 0. 0. 0. 0.
  6  .296471 4.533219 -2.270982 1.068627 -0.036391 0.022261
  9. 4. 1. 0. 0. 0. 0. 0. 0. 0. 0.
  6  .296471 4.533219 -2.270982 1.068627 -0.036391 0.022261
  0. 0. 0. 0. 0. 0. 0. 0. 0. 0.
  #60|30|60
  1 0. 0. 0.
'DRIFT'
  27.5
'FIT'
   2
  5  5 0.  0.2
  7  5 0.  0.2
  2                     r12=0 and r34=0 at focus
1  1  2 8  0.   1.0  0
1  3  4 8  0.   1.0  0
'END'
```

2.2 Adjusting transport at final focus

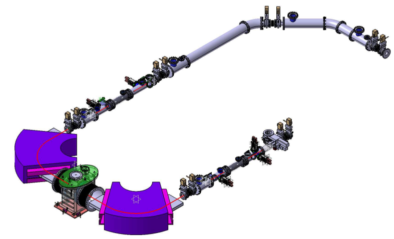

I now constrain R11, R22, R33, R44 to 1,
using MQ1, MQ2, FQ1 coupled with respectively MQ3, MQ4, FQ2.

Bends are simulated with "BEND", they have $\lambda = 8$ cm field fall-off.

This yields the following :

$$MQ1, MQ3/-680.86, \quad MQ2, MQ4/+770.60, \quad FQ1, FQ2/-858.60$$

H and V foci downstream of MQ2 are shifted in this process since MQ1, MQ2 have been used as adjustment variables with no more constraint on R12, R34 at first focus. Transport matrix at the first focus is now :

```
Reference particle (# 1), path length :   116.50000     cm  relative momentum :       1

  -1.307502E-03    0.135140          0              0               0               0
  -7.35987        -4.11945           0              0               0               0
      0               0          -2.50798        6.983367E-02        0               0
      0               0          -6.26123       -0.224386            0               0
      0               0              0              0               1               0
      0               0              0              0               0               1

          DetY-1 =          0   00392,    DetZ-1 =      -   0   03298

          R12=0 at   0.3281E-01 m,        R34=0 at   0.3112     m
```

Transport matrix at the middle of the multipole features the expected R22, R34, R43 zeroed :

```
Reference particle (# 1), path length :   502.01769     cm  relative momentum :       1

   -28.7383         -15.5527             0              0               0           2.40389
     6.429774E-02   -6.122880E-08        0              0               0           1.72654
        0                0            6.48363       -4.006136E-06       0              0
        0                0          -8.123932E-07   0.154235          0              0
   -49.7724        -26.8524              0              0               1           0.485177
        0                0               0              0               0              1

          DetY-1 =      0.0000049309,    DetZ-1 =      -0.0000003309
          R12=0 at  -0.2540E+09 m,        R34=0 at   0.2597E-04 m
```

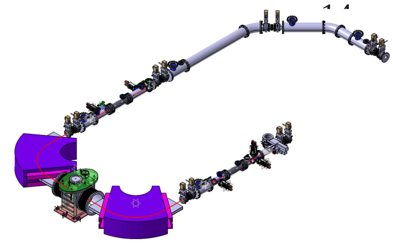

Matrix at final focus does get R11, R22 -1,
R33, R44 close to 1,
with as a subproduct (R21*R12)=0, (R43*R34)=0 since
the determinant is 1, and in addition by symmetry of the line R12 and R34 zero :

```
Reference particle (# 1), path length :   1004.0354     cm  relative momentum :       1

                  TRANSFER  MATRIX  ORDRE  1  (MKSA units)
```

-1	2.045844E-06	0	0	0	-53.7181
-3.69561	-0.999996	0	0	0	-99.2546
0	0	0.993529	9.467627E-05	0	0
0	0	0.248026	1.00654	0	0
-99.2357	-53.7048	0	0	1	9.27083
0	0	0	0	0	1

```
          DetY-1 =       0.0000067474,    DetZ-1 =      -0.0000007106
          R12=0 at   0.2046E-05 m,        R34=0 at  -0.9406E-04 m
```

Zgoubi data file, from object to mid-plane

```
hrsdesir U180_V4
 'OBJET'                                                        1
405.179    (Sn132+, 60 KeV)
5
0.01  .01  0.01  .01  .001  .001
0.  0.  0.  0.  0.  1.
 'PARTICUL'                                                     2
122957.21  1.602176487E-19 0.0 0.0 0.0
 'MARKER'                                                       3
 'DRIFT'                                                        4
42.
 'ELMULT'                                                       5
0
18.5 2. 0. -699.3407339 0. 0. 0. 0. 0. 0. 0. 0.
9. 4. 1. 0. 0. 0. 0. 0. 0. 0. 0.
6  .296471 4.533219 -2.270982 1.068627 -0.036391 0.022261
9. 4. 1. 0. 0. 0. 0. 0. 0. 0. 0.
6  .296471 4.533219 -2.270982 1.068627 -0.036391 0.022261
0. 0. 0. 0. 0. 0. 0. 0. 0. 0.
#60|30|60
1  0. 0. 0.
 'DRIFT'                                                        6
10.00
 'ELMULT'                                                       7
0
18.5 2. 0. +866.6614611  0. 0. 0. 0. 0. 0. 0. 0.
9. 4. 1. 0. 0. 0. 0. 0. 0. 0. 0.
6  .296471 4.533219 -2.270982 1.068627 -0.036391 0.022261
9. 4. 1. 0. 0. 0. 0. 0. 0. 0. 0.
6  .296471 4.533219 -2.270982 1.068627 -0.036391 0.022261
0. 0. 0. 0. 0. 0. 0. 0. 0. 0.
#60|30|60
1 0. 0. 0.
 'DRIFT'                                                        8
27.5
 'MATRIX'                                                       9
1  0
 'DRIFT'                                                       10
27.5
 'ELMULT'                                                      11
0
11. 2. 0. 0. 0. 0. 0. 0. 0. 0. 0. 0.
0. 0. 0. 0. 0. 0. 0. 0. 0. 0. 0.
6  .296471 4.533219 -2.270982 1.068627 -0.036391 0.022261
0. 0. 0. 0. 0. 0. 0. 0. 0. 0. 0.
6  .296471 4.533219 -2.270982 1.068627 -0.036391 0.022261
0. 0. 0. 0. 0. 0. 0. 0. 0. 0.
#60|30|60
1 0. 0. 0.
 'DRIFT'                                                       12
6.0
 'ELMULT'                                                      13
0
22. 4. 0. -924.4183541 0. 0. 0. 0. 0. 0. 0. 0.
9. 4. 1. 0. 0. 0. 0. 0. 0. 0. 0.
6  .296471 4.533219 -2.270982 1.068627 -0.036391 0.022261
9. 4. 1. 0. 0. 0. 0. 0. 0. 0. 0.
6  .296471 4.533219 -2.270982 1.068627 -0.036391 0.022261
0. 0. 0. 0. 0. 0. 0. 0. 0. 0.
#60|30|60
1 0. 0. 0.
 'DRIFT'                                                       14
95.5
 'BEND'                                                        15
0
120.2081528  0.  4.774832720
20. 8.      0.62831853
6     0.498959 1.911289 -1.185953 1.630554 -1.082657 0.318111
20. 8.      0.62831853
6     0.498959 1.911289 -1.185953 1.630554 -1.082657 0.318111
.2
3  0.  0.  -0.7853981633
 'DRIFT'                                                       16
75.0
 'ELMULT'                                                      17
0
15. 20. 0. 0. 0.0001 0. 0. 0. 0. 0. 0. 0. 0.
0. 0. 0. 0. 0. 0. 0. 0. 0. 0. 0.
0  0. 0. 0. 0. 0. 0.
0. 0. 0. 0. 0. 0. 0. 0. 0. 0. 0.
0  0. 0. 0. 0. 0. 0.
0. 0. 0. 0. 0. 0. 0. 0. 0. 0.
0.1
1 0. 0. 0.
 'MATRIX'                                                      18
1  0
 'ELMULT'                                                      19
0
15. 20. 0. 0. 0.0001 0. 0. 0. 0. 0. 0. 0. 0.
0. 0. 0. 0. 0. 0. 0. 0. 0. 0. 0.
0  0. 0. 0. 0. 0. 0.
0. 0. 0. 0. 0. 0. 0. 0. 0. 0. 0.
0  0. 0. 0. 0. 0. 0.
0. 0. 0. 0. 0. 0. 0. 0. 0. 0.
0.1
1 0. 0. 0.
 'DRIFT'                                                       20
75.0
 'BEND'                                                        21
0
120.2081528  0.  4.774832720
20. 8.      0.62831853
6     0.498959 1.911289 -1.185953 1.630554 -1.082657 0.318111
20. 8.      0.62831853
6     0.498959 1.911289 -1.185953 1.630554 -1.082657 0.318111
.2
3    0.      0.       -0.7853981633
 'DRIFT'                                                       22
95.5
 'ELMULT'                                                      23
0
22. 4. 0. -924.4183541 0. 0. 0. 0. 0. 0. 0. 0.
9. 4. 1. 0. 0. 0. 0. 0. 0. 0. 0.
6  .296471 4.533219 -2.270982 1.068627 -0.036391 0.022261
9. 4. 1. 0. 0. 0. 0. 0. 0. 0. 0.
6  .296471 4.533219 -2.270982 1.068627 -0.036391 0.022261
0. 0. 0. 0. 0. 0. 0. 0. 0. 0.
#60|30|60
1 0. 0. 0.
 'DRIFT'                                                       24
6.0
 'ELMULT'                                                      25
0
11. 2. 0. 0. 0. 0. 0. 0. 0. 0. 0. 0.
0. 0. 0. 0. 0. 0. 0. 0. 0. 0. 0.
0  0. 0. 0. 0. 0. 0.
0. 0. 0. 0. 0. 0. 0. 0. 0. 0. 0.
0  0. 0. 0. 0. 0. 0.
0. 0. 0. 0. 0. 0. 0. 0. 0. 0.
0.1
1 0. 0. 0.
 'DRIFT'                                                       26
27.5
 'DRIFT'                                                       27
27.5
 'ELMULT'                                                      28
0
18.5 2. 0. +866.6614611 0. 0. 0. 0. 0. 0. 0. 0.
9. 4. 1. 0. 0. 0. 0. 0. 0. 0. 0.
6  .296471 4.533219 -2.270982 1.068627 -0.036391 0.022261
9. 4. 1. 0. 0. 0. 0. 0. 0. 0. 0.
6  .296471 4.533219 -2.270982 1.068627 -0.036391 0.022261
0. 0. 0. 0. 0. 0. 0. 0. 0. 0.
#60|30|60
1 0. 0. 0.
 'DRIFT'                                                       29
10.00
 'ELMULT'                                                      30
0
18.5 2. 0. -699.3407339 0. 0. 0. 0. 0. 0. 0. 0.
9. 4. 1. 0. 0. 0. 0. 0. 0. 0. 0.
6  .296471 4.533219 -2.270982 1.068627 -0.036391 0.022261
9. 4. 1. 0. 0. 0. 0. 0. 0. 0. 0.
6  .296471 4.533219 -2.270982 1.068627 -0.036391 0.022261
0. 0. 0. 0. 0. 0. 0. 0. 0. 0.
#60|30|60
1  0. 0. 0.
 'DRIFT'                                                       31
42.
 'MATRIX'                                                      32
1   0
 'FIT'                                                         33
3
5   5  30.005  0.105
7   5  28.005  0.105
13  5  23.005  0.105
7
1 2 2 17 0. 1. 0
1 3 4 17 0. 1. 0
1 4 3 17 0. 1. 0
1  1  1   31  -1.   .1  0
1  2  2   31  -1.   .1  0
1  3  3   31   1.   .1  0
1  4  4   31   1.   .1  0
 'END'                                                         34
```

3 Simulating bends by means of field maps

Field across bend edge in tmag3.map field map :

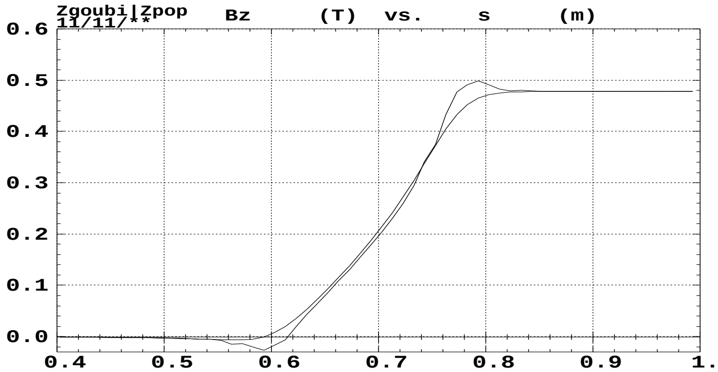

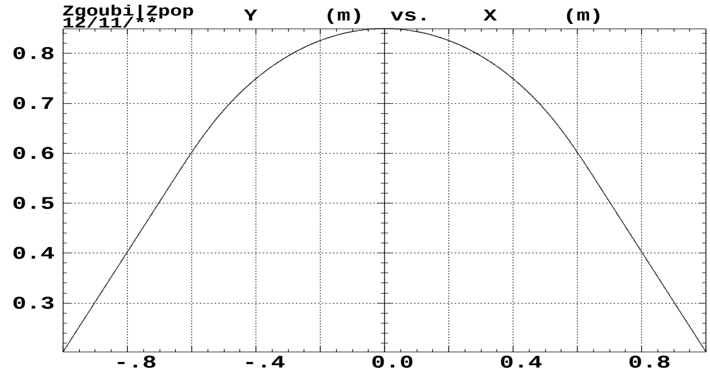

Tansport matrix of the magnet :

```
Reference particle (# 1), path length :   133.53295     cm  relative momentum :       1

 0.731903      0.846525           0             0            0          0.848551
-0.547007      0.732428           0             0            0          1.73518
    0             0           -5.226E-02     1.34173         0             0
    0             0           -0.743281    -5.208E-02        0             0
 1.73190       0.845031           0             0            1          0.488222
```

Theoretical value, hard edge model :

$r11 = \frac{\cos(\phi-\alpha)}{\cos(\alpha)} = \mathbf{0.72654}$ $r12 = r * \sin\phi = \mathbf{0.85}$ $r13 = r * (1 - \cos\phi) = \mathbf{0.85}$

$r21 = -\frac{\sin(\phi-\alpha-\beta)}{\cos(\alpha)\cos(\beta)}/r = \mathbf{-0.55545}$ $r22 = \frac{\cos(\phi-\beta)}{\cos(\beta)} = \mathbf{0.72654}$ $r23 = \sin\phi + (1 - \cos\phi)\tan(\beta) = \mathbf{1.7265}$

$r33 = 1 - \phi * \tan(\alpha) = \mathbf{-0.14125}$ $r34 = r\phi = \mathbf{1.3351}$

$r43 = (-\tan(\alpha) - \tan(\beta) + \phi * \tan(\alpha)\tan(\beta))/r = \mathbf{-0.73402}$ $r44 = 1 - \phi * \tan(\beta) = \mathbf{-0.14125}$

4 “hrs_U180_v6t4.dat”, bends using “tmag4.map”

• The two bends are identical,
• They have R=4m entrance and exit face curvature for compensation of dipole-induced second order aberration.

4.1 Adjusting transport at final focus

R11, R22, R33, R43 at final focus are constrained to ± 1, varying MQ1/3, MQ2/4, FQ1/2.
This yields the following :

$$MQ1, MQ3/-619.12, \quad MQ2, MQ4/+621.8, \quad FQ1, FQ2/-298.7$$

• V focus downstream of MQ1, MQ2 are shifted in the process, respectively 0.2 m and 5.2 m. Transport matrix at the first focus is now :

```
Reference particle (# 1), path length :   116.50000     cm  relative momentum :       1

      0.674029        0.561720            0               0               0               0
      -5.06905        -2.74079            0               0               0               0
          0               0          -1.98854        0.184725             0               0
          0               0          -5.03410       -3.524032E-02         0               0

          DetY-1 =       0.0000081748,    DetZ-1 =      -0.0000009083
          R12=0 at   0.2049     m,        R34=0 at    5.242     m
```

• ing at final focus :

```
Reference particle (# 1), path length :   1004.0393     cm  relative momentum :    1.00000

     -0.996940        5.047192E-03        0              0              0.00000        -25.5558
      -3.83735       -0.990415            0              0              0.00000        -49.1183
          0               0           0.992267      -4.150674E-04       0.00000            0
          0               0            34.7231       0.992423           0.00000            0
      -48.9741        -25.4911            0              0              1.00000         9.33369

          DetY-1 =        0.0067518362,    DetZ-1 =      -0.0008391665
          R12=0 at   0.5096E-02 m,         R34=0 at   0.4182E-03 m
```

4.2 Tracking through “hrs_U180_v6t4”

Three momenta, observed at mid-plane and final-focus

The object used is 1π mm.mrad in both planes (the initial YY’ and ZZ’ distributions are plotted in Fig. 6), with three momenta at $\Delta p/p = 0, \pm 0.0005$, all three with momentum spread $\delta p/p = 0$.

The images at mid-plane and at final-focus are shown in respectively Figs. 7, 8.

Zgoubi data :

```
 'MCOBJET'          1
 409.3505601114    (Sn132+, 60 KeV)
2
2000
2      2      2     2      1     1
0.     0.     0.    0.     0.    1.
1      1      1     1      1     3
0.     0.     0.    0.     0.    0.0005
.5e-3 2.e-3 .5e-3  2.e-3   0.   .0
4      4      4     4      1     1
1 0. 0. 0. 0.
 123456 234567 345678
```

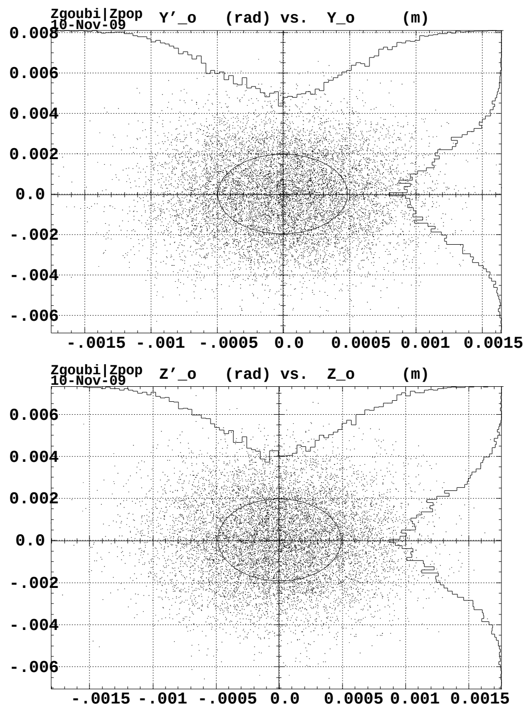

Figure 6: YY’ and ZZ’ distributions at beginning of hrs_u180_v6t4.

MID-PLANE

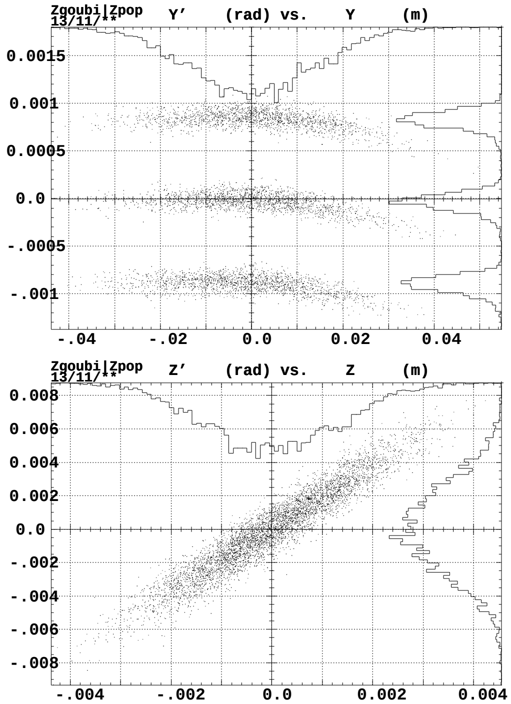

Figure 7: Observation of three momenta at mid-plane of hrs_u180_v6t4.
$\Delta p/p = 0, \ \pm 0.0005$**, H and V phase-spaces, 5000 particles.**
Effect of strong second order aberration (Y/θ^2) **is noticeably damped.**

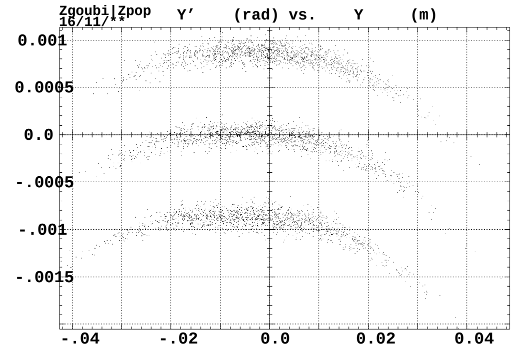

Figure 8: For comparison : Bend with straight faces (no second order compensation), using “hrs_U180_v6t3.dat” with “tmag3.map” field map.

FINAL FOCUS

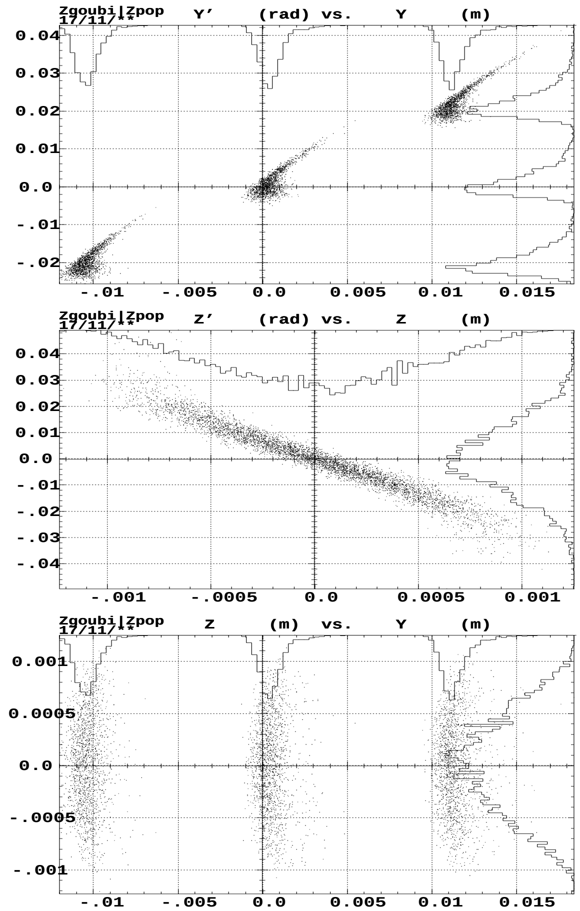

Figure 9: **Three momenta at final focus of hrs_u180_v6t4.**

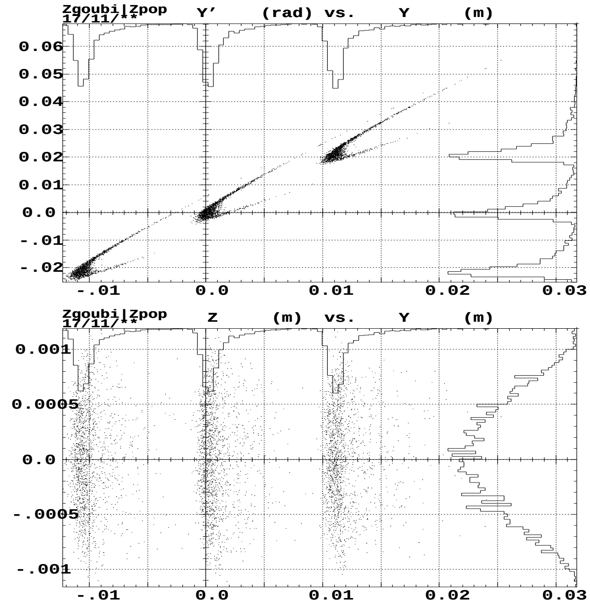

Figure 10: **For comparison : straight Bend faces (no second order face curvature).**

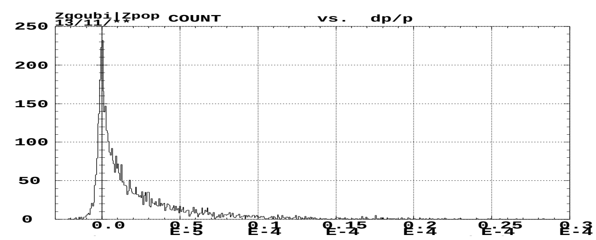

Figure 11: **Note momentum spread induced by electrostatic lenses.**